



Arrangement of Monofunctional Silane Molecules on Silica Surfaces: Influence of Alkyl Chain Length, Head-Group Charge, and Surface Coverage, from Molecular Dynamics Simulations, X-ray Photoelectron Spectroscopy, and Fourier Transform Infrared Spectroscopy

Solène Lecot, Antonin Lavigne, Zihua Yang, Thomas Gehin, Claude Botella, Vincent Jousseau, Yann Chevolot, Magali Phaner-Goutorbe, Christelle Yeromonahos

► To cite this version:

Solène Lecot, Antonin Lavigne, Zihua Yang, Thomas Gehin, Claude Botella, et al.. Arrangement of Monofunctional Silane Molecules on Silica Surfaces: Influence of Alkyl Chain Length, Head-Group Charge, and Surface Coverage, from Molecular Dynamics Simulations, X-ray Photoelectron Spectroscopy, and Fourier Transform Infrared Spectroscopy. *Journal of Physical Chemistry C*, 2020, 124 (37), pp.20125-20134. 10.1021/acs.jpcc.0c05349 . hal-03214427

HAL Id: hal-03214427

<https://hal.science/hal-03214427>

Submitted on 1 May 2021

HAL is a multi-disciplinary open access archive for the deposit and dissemination of scientific research documents, whether they are published or not. The documents may come from teaching and research institutions in France or abroad, or from public or private research centers.

L'archive ouverte pluridisciplinaire **HAL**, est destinée au dépôt et à la diffusion de documents scientifiques de niveau recherche, publiés ou non, émanant des établissements d'enseignement et de recherche français ou étrangers, des laboratoires publics ou privés.

C: Surfaces, Interfaces, Porous Materials, and Catalysis

Arrangement of Monofunctional Silane Molecules on Silica Surfaces: Influence of the Alkyl Chain Length, Head-Group Charge and Surface Coverage, from Molecular Dynamics Simulations, X-Ray Photoelectron Spectroscopy and Fourier Transform Infrared Spectroscopy Analysis.

Solène Lecot, Antonin Lavigne, Zihua Yang, Thomas Géhin, Claude Botella, Vincent Jousseau, Yann Chevolot, Magali Phaner-Goutorbe, and Christelle Yeromonahos

J. Phys. Chem. C, **Just Accepted Manuscript** • DOI: 10.1021/acs.jpcc.0c05349 • Publication Date (Web): 21 Aug 2020

Downloaded from pubs.acs.org on August 25, 2020

Just Accepted

"Just Accepted" manuscripts have been peer-reviewed and accepted for publication. They are posted online prior to technical editing, formatting for publication and author proofing. The American Chemical Society provides "Just Accepted" as a service to the research community to expedite the dissemination of scientific material as soon as possible after acceptance. "Just Accepted" manuscripts appear in full in PDF format accompanied by an HTML abstract. "Just Accepted" manuscripts have been fully peer reviewed, but should not be considered the official version of record. They are citable by the Digital Object Identifier (DOI®). "Just Accepted" is an optional service offered to authors. Therefore, the "Just Accepted" Web site may not include all articles that will be published in the journal. After a manuscript is technically edited and formatted, it will be removed from the "Just Accepted" Web site and published as an ASAP article. Note that technical editing may introduce minor changes to the manuscript text and/or graphics which could affect content, and all legal disclaimers and ethical guidelines that apply to the journal pertain. ACS cannot be held responsible for errors or consequences arising from the use of information contained in these "Just Accepted" manuscripts.

Arrangement of Monofunctional Silane Molecules
on Silica Surfaces: Influence of the Alkyl Chain
Length, Head-Group Charge and Surface Coverage,
from Molecular Dynamics Simulations, X-Ray
Photoelectron Spectroscopy and Fourier Transform
Infrared Spectroscopy Analysis.

*Solène Lecot[§], Antonin Lavigne[§], Zihua Yang[§], Thomas Géhin[§], Claude Botella[§], Vincent
Jousseau[⊥], Yann Chevolot[§], Magali Phaner-Goutorbe[§], Christelle Yeromonahos^{§*}*

[§] Université de Lyon, Institut des Nanotechnologies de Lyon UMR 5270, Ecole Centrale de
Lyon, 36 avenue Guy de Collongue, 69134 Ecully, France

[⊥] Université Grenoble Alpes, CEA, LETI, F-38000 Grenoble, France

*** Corresponding Author**

Christelle Yeromonahos: christelle.yeromonahos@ec-lyon.fr, + 33 4 72 18 62 35

ABSTRACT

Surface chemical functionalization is used in analytical tools to immobilize biomolecules that will capture a specific analyte, but also to reduce the nonspecific adsorption. Silane monolayers are widely used to functionalize silica surfaces. Their interfacial properties are linked to the silane organization. Here we study, by Molecular Dynamics simulations, the effects of silane molecule headgroup charge, alkyl chain length, and surface coverage on the structure of silane monolayers. Four molecules are investigated: 3-aminopropyldimethylethoxysilane, n-propyldimethylmethoxysilane, octadecyldimethylmethoxysilane, tert-butyl-11-(dimethylamino(dimethyl)silyl)undecanoate. The results suggest that, while long alkyl chains straighten out and adopt a more organized structure as surface coverage increases, the tilt angle of short chains is independent from surface coverage. Furthermore, in the case of long alkyl chains, a charged headgroup seems to reduce the tilt angle to surface coverage dependence. The simulated alkyl chain tilt angles were qualitatively validated by infrared spectroscopy and X-ray photoelectron spectroscopy. Also, a hexagonal packing is observed in all the monolayers, but is more defined as surface coverage increases. The nematic order parameter suggests that this packing is governed by the parallel orientation of the first C-C bonds near the surface. So, even short alkyl chains, with a large tilt angle distribution, present a hexagonal packing.

Introduction

A large number of applications takes advantage of surface chemical functionalization. In particular, in the field of biosensing, the specificity of the device (the fact of capturing solely a given analyte) and the signal to noise ratio are related to surface chemistry. For example, surface chemical functionalization allows the immobilization of biomolecules that will capture specifically biomarkers (peptides, proteins, DNA) or whole organisms for diagnosis purposes.¹⁻⁶ The background signal can also be reduced thanks to the chemical functionalization of material surfaces allowing the reduction of non-specific adsorption. Among the various chemical functionalizations, silane molecules have been widely used for the modification of oxides, especially oxidized silicon surfaces (SiO_2).^{2,3,7-9}

The structure, organization and surface energies of various silane modified SiO_2 surfaces have been studied by various characterization techniques as a function of experimental parameters, in particular in the case of multifunctional silane monolayers. Atomic Force Microscopy (AFM) experiments suggested that, after deposition on SiO_2 surface, silane molecules can diffuse laterally to self-assemble either into fractal network or into liquid phase state, depending on external parameters such as temperature.¹⁰ Also, AFM studies have established that the strength of hydrophobic interactions on a silane monolayer is strongly related to the order of the silane molecules.¹¹ Indeed, pull-off forces resulting from hydrophobic adhesion are higher on crystalline-like monolayers than on liquid-like monolayers. The structure of *n*-alkane monolayers, with $n > 12$, has been extensively studied by Fourier Transform Infra-Red (FTIR) and X-Ray Diffraction (XRD) measurements.¹²⁻¹⁷ While the positions of the methyl and methylene vibration modes from FTIR spectra yielded information on the presence of gauche defects in the alkyl chains and on the average alkyl chain tilt angle, the molecule crystalline packing inside the monolayer was addressed

by XRD measurements. Hexagonal crystalline-like domains with an intermolecular in-plane distance of 4.7-5 Å were observed for monolayers of *n*-alkylsilane molecules with $n > 14$.^{13,16} Shorter *n*-alkylsilane monolayers were shown to present more gauche defects than the longer ones, but also a lower surface coverage.¹² Also, in the case of multifunctional silane molecules, a Multiple Transmission and Reflection Infra-Red Spectroscopy study shown that the nature of the leaving groups (Si(OMe)₃, Si(OEt)₃, Si(Cl)₃) controls the rate of their hydrolysis, leading to very different monolayer structures.¹⁷

As the surface coverage cannot easily be varied experimentally, Molecular Dynamics (MD) simulations are well suited to study the combined effects of surface coverage and alkyl chain length of silane molecules on alkyl chain tilt angle, gauche defects and nematic order parameter. However, only few MD simulations studies have addressed these questions. Different MD studies suggested that the order parameter of *n*-alkylsilane monolayers (for $n > 8$) increases as the alkyl chain length and the surface coverage increase, while alkyl chain tilt angles are independent of chain length and decrease as surface coverage increases.¹⁸⁻²² Among them, it was also shown that perfluorodecyltrichlorosilane (FDTS) monolayers at high surface coverage present a hexagonal packing, whereas such packing was attenuated for octadecyltrichlorosilane (OTS) monolayers for the same surface coverage.¹⁸ In the present study, we demonstrate an effect of the head-group charge and alkyl chain length ($n < 18$), on the organization of the monolayer.

We propose a MD simulation study on the effects of head-group charge (positive, neutral and negative), alkyl chain length (n from 3 to 18), and surface coverage (1.5 to 4.2 nm⁻²) on the structure of silane monolayers. The four different silane molecules are 3-aminopropyldimethylethoxysilane (C₇H₁₉NOSi named NH₃⁺), n-propyldimethylmethoxysilane (C₆H₁₆OSi named CH₃ short), octadecyldimethylmethoxysilane (C₂₁H₄₆OSi named CH₃ long), and

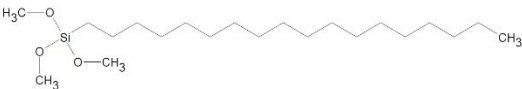
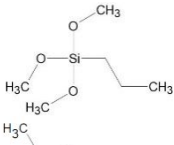
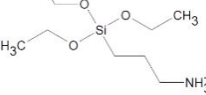
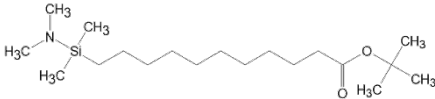
tert-butyl-11-(dimethylamino(dimethyl)silyl)undecanoate ($C_{19}H_{41}NO_2Si$, leading to COO^- after deprotection) (Table 1). The different silane monolayers were characterized by the alkyl chain tilt angle, the average number of gauche defects in the alkyl chains, the nematic order parameter for each C-C bond and its overall distribution, and the hexagonal packing of silane molecules on SiO_2 surface and its persistence length. To check that the simulated morphologies were consistent with experimental evidences, alkyl chain tilt angles were compared to experimental values obtained from FTIR-Attenuated Total Reflectance (FTIR-ATR) measurements. To this aim, four silane monolayers (one per silane molecule type) were elaborated from a liquid phase process on SiO_2 surfaces. The surface coverages were estimated by X-ray Photoelectron Spectroscopy (XPS) analysis.

1. Materials and methods

1-1. Experimental materials and methods

Materials. SiO_2 (20 nm) / Aluminium (200 nm) / Silicon substrates were prepared by Physical Vapor Deposition (PVD) using a 200 mm Applied Materials Endura 5500 platform. The depositions were performed on Si (100) wafers without air break between Aluminium and SiO_2 . 3-aminopropyldimethylethoxysilane 95% (NH_3^+), n-propyldimethylmethoxysilane 95% (CH_3 short) and octadecyldimethylmethoxysilane 95% (CH_3 long) were purchased from ABCR. Tert-butyl-11-(dimethylamino(dimethyl)silyl)undecanoate (leading to COO^- after deprotection) was synthesized accordingly to a protocol previously reported.²³ The chemical structures of the four molecules are shown in Table 1.

Table 1. The different silane molecules and surface coverage studied.

	Designation of silane molecule	Silane structural formula	Surface coverage used in MD simulations (nm ⁻²)	Surface coverage estimated by XPS analysis (nm ⁻²)
Systems with silane layer	CH ₃ long		1.5 – 3.0 – 4.2	3
	CH ₃ short		1.5 – 3.0 – 4.2	3
	NH ₃ ⁺		3.0	8
	COO ⁻		3.0 – 4.2	3
System without silane layer		Bare SiO ₂		

Chemical surface functionalization. The substrates were cleaned by ozone/Ultraviolet treatment under oxygen flow for 30 min to remove organic contamination and to obtain a hydroxyl-terminated surface. Next, the substrates were heated at 150°C for 4 hours under nitrogen, allowed to cool to room temperature under nitrogen and then, the substrates were immersed in 10 ml dried pentane containing 90 µl of silane molecules. After 1 hour of incubation, the pentane was evaporated and the samples were heated at 150°C for 15 hours, to allow the silanization reaction. Finally, the samples were washed 10 minutes in tetrahydrofurane (THF) under sonication, and 10 minutes in ultrapure water under sonication.

XPS analysis. XPS measurements were performed using a VSW spectrometer equipped with a monochromatized X-ray source (Al K α 1486.6 eV) in which the angle between the incident beam and the detector was the magic angle. The angular resolution was 3°. Take-off angle was 90° relative to the substrate surface. The energetic resolution was 0.2 eV. The data analysis was performed with CasaXPS software. Si(-O)₄ binding energy was set at 104 eV. A Shirley background was subtracted on Si2p and O1s spectra when coming from bulk elements while a linear background was subtracted on C1s spectra as surface elements. Peaks were fitted by a Gauss-Lorentz curve.

FTIR-ATR analysis. FTIR-ATR was performed using a Thermo Nicolet 6700 spectrometer with a Mercury-Cadmium-Telluride (MCT) detector and a diamond crystal from 800 to 3000 cm⁻¹. Results were obtained by averaging 256 scans with a resolution of 4 cm⁻¹.

1-2. Computational methods

System description. The silane molecules used are those presented in Table 1, after hydrolyzation, based on a trisilanol structure with two silanol groups remaining unreacted to behave similarly to a monofunctional silane (dimethylsilanol structure), as already reported in a previous study.²⁴ Such a structure was used because its force field is already known¹⁸, whereas the force field of dimethylsilanol is not published. The systems were built following the method proposed by Roscioni *et al.*¹⁸ Silane molecules were initially randomly positioned on an amorphous SiO₂ surface, without explicit bonding between silane molecules and the surface, allowing their spontaneous lateral organization. As surface roughness has a strong influence on the lateral organization of silane molecules²⁵, the parameters of amorphous SiO₂ surface published by Roscioni *et al.*¹⁸ were used. Indeed, its Root Mean Square (RMS) value is close to the experimental

1
2
3 value of SiO₂ thin films. Figure 1 illustrates the arrangement of the silane molecules on SiO₂
4
5 surface after 100-ns MD simulations. The simulation box included water molecules with the model
6
7 TIP4P. The charges of the silane head-groups were compensated with counterions (Na⁺ or Cl⁻) at
8
9 a concentration of 150 mM to mimic physiological conditions. A Lennard-Jones (LJ) wall was
10
11 added at the top of the box to avoid interactions between water and the bottom side of the SiO₂
12
13 surface and to prevent any surface curvature.²⁶ The simulation box included nearly 100 000 atoms
14
15 and its dimensions are 7.8 nm x 7.8 nm x 15 nm.
16
17
18
19
20
21
22
23
24
25
26
27
28
29
30
31
32
33
34
35
36
37
38
39
40
41
42
43
44
45
46
47
48
49
50
51
52
53
54
55
56
57
58
59
60

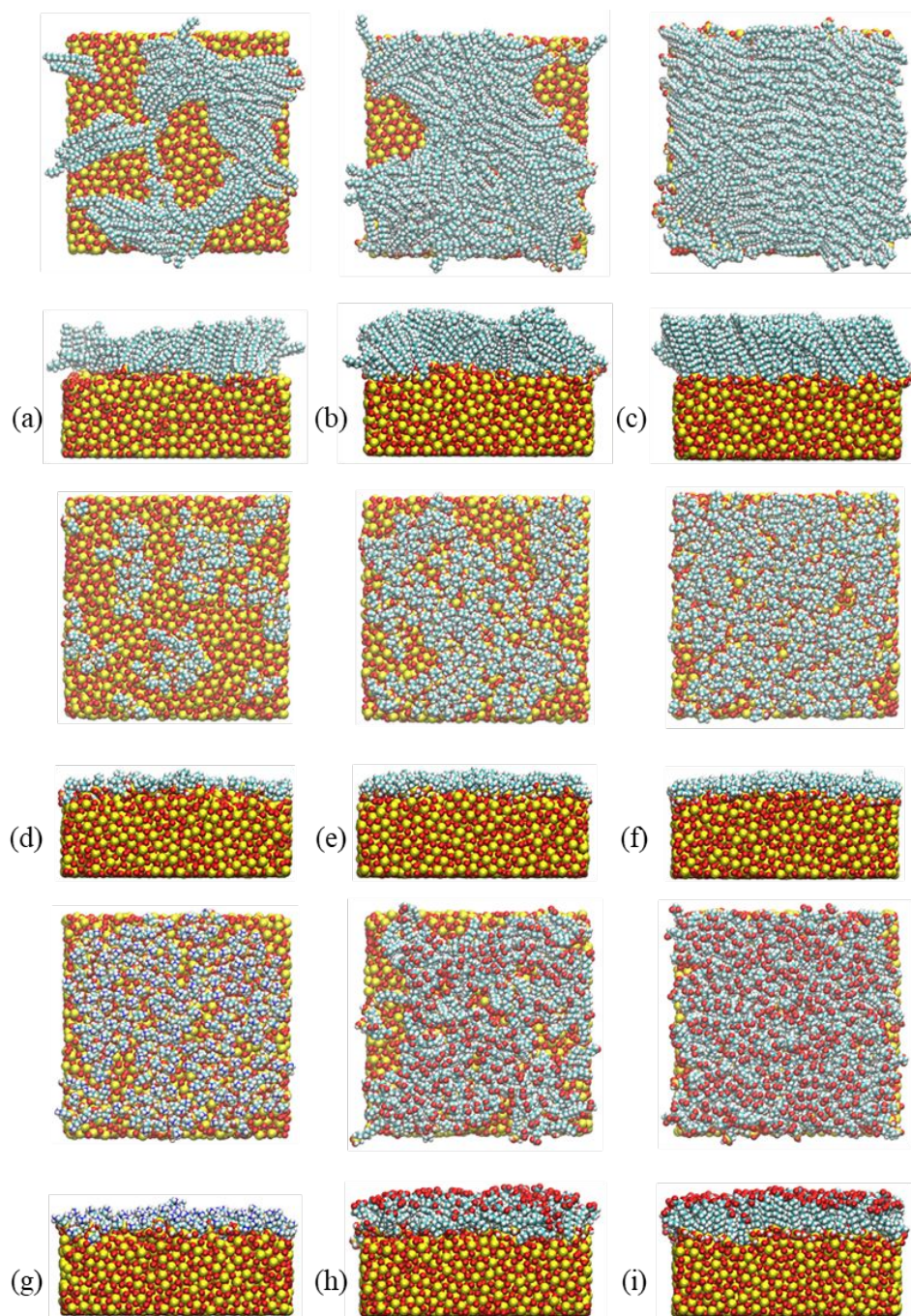


Figure 1. Arrangement of silane molecules on the amorphous SiO_2 layer after 100 ns MD simulation for different silane head-groups, alkyl chain lengths and surface coverages : (a) CH_3 long $c = 1.5 \text{ nm}^{-2}$, (b) CH_3 long $c = 3.0 \text{ nm}^{-2}$, (c) CH_3 long $c = 4.2 \text{ nm}^{-2}$, (d) CH_3 short $c = 1.5 \text{ nm}^{-2}$, (e) CH_3 short $c = 3.0 \text{ nm}^{-2}$, (f) CH_3 short $c = 4.2 \text{ nm}^{-2}$, (g) NH_3^+ $c = 3.0 \text{ nm}^{-2}$, (h) COO^- $c = 3.0$

nm⁻² and (i) COO⁻ c = 4.2 nm⁻². Atoms are shown in yellow (silicon), red (oxygen), cyan (carbon), white (hydrogen) and blue (nitrogen).

Simulation details. All the simulations were performed with the Gromacs simulation package, version 5.1.3²⁷ and the VMD software package version 1.9.3²⁸ was used for visualization. Firstly, energy minimization was applied to the system using the Steepest Descent Minimization method. Then, NVT and NPT equilibrations were carried during 100 ps each, and production simulations were performed for 100 ns. A leap-frog algorithm was used for integration of the equations of motion with a time step of 2 fs. Constraints were applied to bond parameters with a LINCS algorithm. The temperature was maintained at 300 K with a Nose-Hoover thermostat using a time constant of 0.4 ps and the pressure was kept at 1 bar with a Parrinello-Rahman barostat using a time constant of 2 ps. Water and ions were both described with OPLS all-atom force-field.²⁹ The parameters to describe the LJ wall were taken from a previous study.²⁶ Force-field for both silane molecules and SiO₂ surfaces were adapted from recent studies^{18,19}, and from the OPLS²⁹ all-atom force field. LJ potentials were truncated with a cut-off distance of 1 nm. Long range electrostatic interactions were calculated with the Particle Mesh Ewald method and a cut-off of 1 nm.

Analysis parameters. The following parameters were evaluated by using Gromacs functions, VMD tools and home-made Python codes. The errors bars were estimated using the standard deviation. The curves and histograms were fitted using Bézier functions.

Tilt angles. The alkyl chain tilt angle is defined as the angle α between the normal to the SiO₂ surface and the vector between the silicon and terminal atoms of the silane molecule.¹⁸

Gauche defects. Gauche defect parameter was evaluated as the proportion of C-C-C-C torsion angles in *trans* conformation.³⁰ For each silane molecule, we calculated all its C-C-C-C torsion

angle ϕ . If $150^\circ \leq \phi \leq 180^\circ$, the angle is in *trans* conformation and if $50^\circ \leq \phi \leq 150^\circ$, the angle is in *gauche* conformation. Gauche defect parameter is the ratio r_{trans} between the number of *trans* conformations and the total of *trans* and *gauche* conformations.

Nematic order parameter. The chemical bond order parameter S_2^i describes the orientation of the i^{th} chemical bond, in a silane molecule, relative to the surface normal.³⁰ It is defined as:

$$S_2^i = \frac{3 \cos^2 \varphi_i - 1}{2}$$

where φ_i is the angle between the i^{th} C-C bond and the surface normal. S_2^i takes values between -0.5 and 1, where -0.5 corresponds to a bond parallel to the surface and 1 corresponds to a bond perpendicular to the surface. We investigated the $\langle S_2^i \rangle$ value (average on all the silane molecules of S_2^i values for a given i^{th} bond) and the S_2 distribution (probability of each S_2 value independently of the bond number in the alkyl chain). In a group of randomly oriented bonds, $\langle S_2 \rangle = 0$ whereas $\langle S_2^i \rangle = 0$ means that $\langle \varphi_i \rangle = 55^\circ$.

Radial Distribution Function (RDF). The 2D radial distribution of silane molecules was investigated in the (x,y) plane (SiO_2 plane surface), taking into account periodic boundary conditions. It is proportional to the probability of finding the Si atom of a silane neighboring molecule for a given position on the plane, while the Si atom of the reference silane molecule is fixed at origin.^{18,31}

2. Results and Discussion

2.1 MD simulations

Previous studies have shown the effects of alkyl chain length, with more than 6 carbon atoms ($n > 6$), at different surface coverages, on the structural properties of silane monolayers. In this study, we decipher the impact of charged functional head-group and alkyl chain length, with more than 3 carbon atoms ($n > 3$), at different surface coverages, on the structural properties of silane monolayers. MD simulations have been performed for all systems during 100 ns. The silane molecule diffusion distance is stabilized rapidly after 30 ns in all systems (Supporting information, Figure S1). After this diffusion phase, the Si atom of silane molecules can be considered as covalently fixed to the O atom of SiO₂. The alkyl chain tilt angle α , nematic order parameter $\langle S_2 \rangle$ and gauche defect fraction r_{trans} are correlated to the crystal packing of silane molecules. The results are summarized in Table 2.

Table 2. Alkyl chain tilt Angle, Nematic Order Parameter and Gauche Defect Parameter of the Silane Monolayers Studied.

System		Alkyl chain tilt angle ^(a)		Nematic order parameter $\langle S_2 \rangle$		Gauche defect parameter
		α (°)	FWHM ^(b) (°)	Even bond	Odd bond	r_{trans}
CH ₃ long	$c = 1.5 \text{ nm}^{-2}$	40	38	0.05	0.03	0.81
	$c = 3.0 \text{ nm}^{-2}$	34	26	0.06	0.22	0.85
	$c = 4.2 \text{ nm}^{-2}$	32	24	0.04	0.40	0.89
CH ₃ short	$c = 1.5 \text{ nm}^{-2}$	22	53	-0.04	0.32	(c)
	$c = 3.0 \text{ nm}^{-2}$	22	35	-0.04	0.42	(c)
	$c = 4.2 \text{ nm}^{-2}$	22	32	-0.03	0.53	(c)
NH ₃ ⁺	$c = 3.0 \text{ nm}^{-2}$	23	57	0.17	0.05	(c)
COO ⁻	$c = 3.0 \text{ nm}^{-2}$	19	27	0.20	0.16	0.69
	$c = 4.2 \text{ nm}^{-2}$	20	30	0.26	0.23	0.70

(a) Tilt angle distribution are depicted in Supporting Information, Figure S2. (b) Full Width at Half Maximum (FWHM). (c) r_{trans} value is not relevant for small molecules with only one torsion angle.

Tilt angle. As shown in Table 2 (and Figure S2 in Supporting Information), the average tilt angle of CH_3 long molecules increases from 32° to 40° , while the Full Width at Half Maximum (FWHM) of the tilt angle distribution increases from 24° to 38° , as the surface coverage decreases from 4.2 nm^{-2} to 1.5 nm^{-2} . This indicates that CH_3 long molecules straighten out and adopt a more organized structure, as the coverage increases. These results are in agreement with previous MD studies, for long alkyl chains ($n > 8$)¹⁸⁻²⁰, and can be explained by an increase in Van der Waals forces between alkyl chains as their amount increases. However, very short alkyl chains (CH_3 short, NH_3^+ , $n = 3$) seem to behave very differently from long ones ($n > 8$). The average tilt angles of NH_3^+ and CH_3 short molecules seem to be independent of the studied surface coverages and they are similar, around 20° . Furthermore, a charged head-group seems also to influence the tilt angle to surface coverage relationship of silane molecules with long alkyl chains ($n > 8$). Indeed, despite a chain length of eleven carbon atoms ($n = 11$), no influence of surface coverage was observed on the tilt angle of COO^- silane molecules. Regarding on NH_3^+ and COO^- molecules, repulsion between their charged functional head-groups can explain the widening in their tilt angles distribution. The tilt angle distribution of CH_3 short is larger than for CH_3 long, and the tilt angle distribution of NH_3^+ is larger than for COO^- at a given surface coverage. It can be explained by the effect of Van der Waals forces between long alkyl chains. These results suggest that the FWHM of tilt angle distributions increases with charged head-groups and decreases as chain length increases.

Moreover, the degree of aggregation of silane molecules (observed on Figure 1), can be related to the FWHM of the tilt angle distribution. Indeed, for a same coverage (*e.g.* $c = 3.0 \text{ nm}^{-2}$), CH_3 long

molecules are positioned within a single and dense aggregate, CH₃ short molecules form several smaller aggregates separated by small non-functionalized SiO₂ areas, and silane molecules with charged head-groups seem more evenly dispersed on the surface. So, both charged head-groups and short alkyl chains seem to decrease silane molecule aggregation on the SiO₂ surface, while increasing the FWHM of the tilt angle distributions. Indeed, the FWHM of the tilt angle is smaller for CH₃ long monolayer (26°) than for CH₃ short (35°) and NH₃⁺ monolayers (57°) (Table 2). Actually, silane molecules within a single dense aggregate could tend to behave similarly to increase Van der Waals interactions (leading to a low FWHM value), while more evenly dispersed silane molecules could be less impacted by the neighboring silane (leading to a high FWHM value). However, COO⁻ and CH₃ long monolayers have similar FWHM (27° and 26° respectively), despite very different surface distributions. This result could be explained by a balance between the opposite effects of the charged head-group and of the long alkyl chain of COO⁻ molecules.

So, the FWHM of the tilt angle distribution of silane molecules seems to depend, in the same way as the degree of dispersion of silane molecules on SiO₂ surface, on the presence of charged head-groups and on the alkyl chain length.

Gauche defects. As shown in Table 2, CH₃ long silane molecules at low surface coverage ($c = 1.5 \text{ nm}^{-2}$) present a lower r_{trans} (0.81), which means that there are more gauche defects, than at higher coverages ($r_{\text{trans}} = 0.85$ and $r_{\text{trans}} = 0.89$ for $c = 3.0 \text{ nm}^{-2}$ and $c = 4.2 \text{ nm}^{-2}$, respectively). These findings are in good agreement with experimental reports found in the literature.^{22,32,33} COO⁻ molecules have more gauche defects than CH₃ long molecules for the same coverage ($r_{\text{trans}} = 0.69$ and $r_{\text{trans}} = 0.7$ for $c = 3.0 \text{ nm}^{-2}$ and $c = 4.2 \text{ nm}^{-2}$, respectively). The presence of charged head-groups results in an increase in gauche defects. As the alkyl chains of NH₃⁺ and CH₃ short silane

1
2
3 molecules contain only one torsion angle, the calculation of their gauche defect parameter is not
4
5 relevant.
6

7
8 **Nematic order parameter.** As discussed above, in our CH₃ long monolayers, alkyl chains tilt
9
10 angles are in the range of 32° to 40°. As a consequence, for perfectly parallel CH₃ long molecules,
11
12 such angles should lead to S_2 values in the range of 0.98 to 1 for each odd bond and in the range
13
14 of -0.24 to -0.4 for each even bond. As the CH₃ long surface coverage increases, the odd bond
15
16 $\langle S_2^{2n+1} \rangle$ value increases from 0.03 to 0.4, as shown in Figure 2. Also, as shown in Figure 3, the S_2
17
18 probability distribution shows that two values for odd and even bonds (1 and -0.25) are more and
19
20 more represented as surface coverage increases. These results reveal that an organization of the
21
22 CH₃ long molecules in a herringbone structure appears as coverage increases, in agreement with
23
24 previous studies.^{18,22,30} Thus, long alkyl chains (without head-groups) and high surface coverage
25
26 lead to a well-ordered state, allowing a preferred alkyl chain orientation with few gauche
27
28 distortions. Regarding CH₃ short monolayers, alkyl chain tilt angles are around 22°. As a
29
30 consequence, for perfectly parallel CH₃ short molecules, such angles should lead to a S_2 value of
31
32 0.94 for the odd bond. Our results show that the CH₃ short odd bond $\langle S_2^1 \rangle$ value is 0.4 at $c = 3.0$
33
34 nm⁻² and 0.53 at $c = 4.2$ nm⁻², which is much higher than the odd bond $\langle S_2^{2n+1} \rangle$ values of CH₃ long
35
36 (respectively 0.2 and 0.4). Even if CH₃ short molecules have a large tilt angle distribution, the
37
38 order parameter relative to their second C-C bond is high, meaning that this C-C bond seems highly
39
40 ordered through the monolayer. In the case of NH₃⁺ and COO⁻ molecules, $\langle S_2^i \rangle$ values are close to
41
42 0 for even as well as for odd bonds, and the herringbone structure is not observed (Figure 2), even
43
44 at high coverage for COO⁻ molecules. All these observations suggest that the presence of charged
45
46 head-groups results in a more disordered monolayer.
47
48
49
50
51
52
53
54
55
56
57
58
59
60

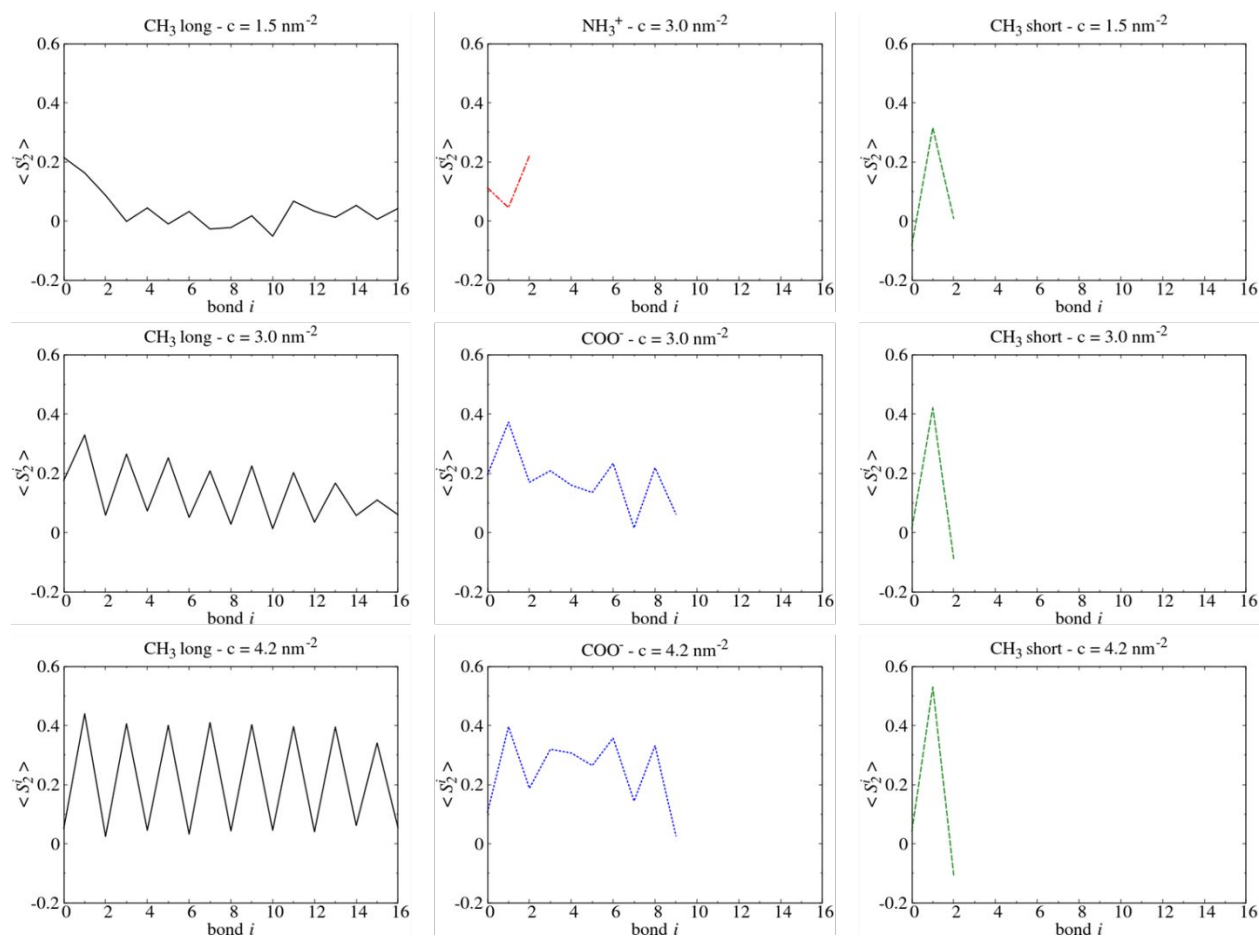


Figure 2. Average nematic order parameter $\langle S_2^i \rangle$ computed for each C-C or C-N bond of the different silane monolayers. Silane molecules present a herringbone structure when $\langle S_2^i \rangle$ varies periodically between odd and even bonds.

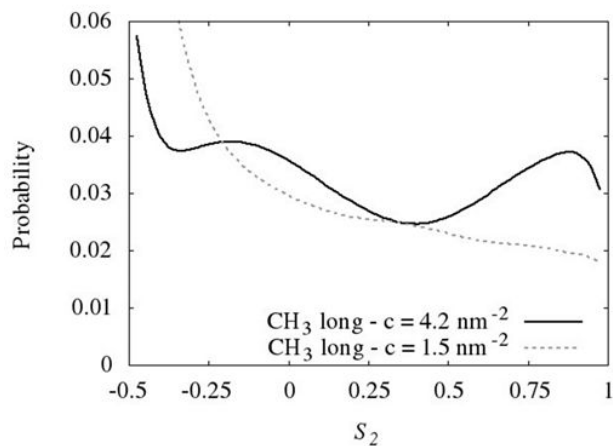


Figure 3. Distribution of the nematic order parameter S_2 for CH_3 long silane monolayer at surface coverage $c = 1.5 \text{ nm}^{-2}$ and $c = 4.2 \text{ nm}^{-2}$. $S_2 = 0$ corresponds to a bond parallel to the surface. For CH_3 long ($c = 4.2 \text{ nm}^{-2}$) values around -0.25 and 1 are more probable, which corresponds to the S_2 values for a tilt angle of 32° .

2D Radial Distribution Function. The high nematic order parameters at high surface coverages for CH_3 long suggest the presence of a positional order in these monolayers. To assess it, the two dimensional Radial Distribution Function (RDF) in the (x,y) plane was calculated.^{18,34} At initial state, because the silane molecules are randomly positioned in the (x,y) plane, the RDF is a line whose slope is directly proportional to the surface coverage (Supporting Information, Figure S3). At final state, all the systems present several peaks, which means that positional order and periodicity appear even for the NH_3^+ silane molecules (Figure 4). As shown in Figure 5, for CH_3 long silane monolayers at $c = 3.0 \text{ nm}^{-2}$ and $c = 4.2 \text{ nm}^{-2}$, the 2D maps of the RDF clearly present a hexagonal packing. This means that each silane molecule has six closest neighbors, spaced by 0.5 nm. For $c = 1.5 \text{ nm}^{-2}$, the hexagonal packing is less obvious and the intensity of the first peak decreases. It can be explained by defects (absence of molecules at some places) in the monolayer due to low surface coverage, as shown in Figure 1. These results are in agreement with previous MD studies.^{18,34}

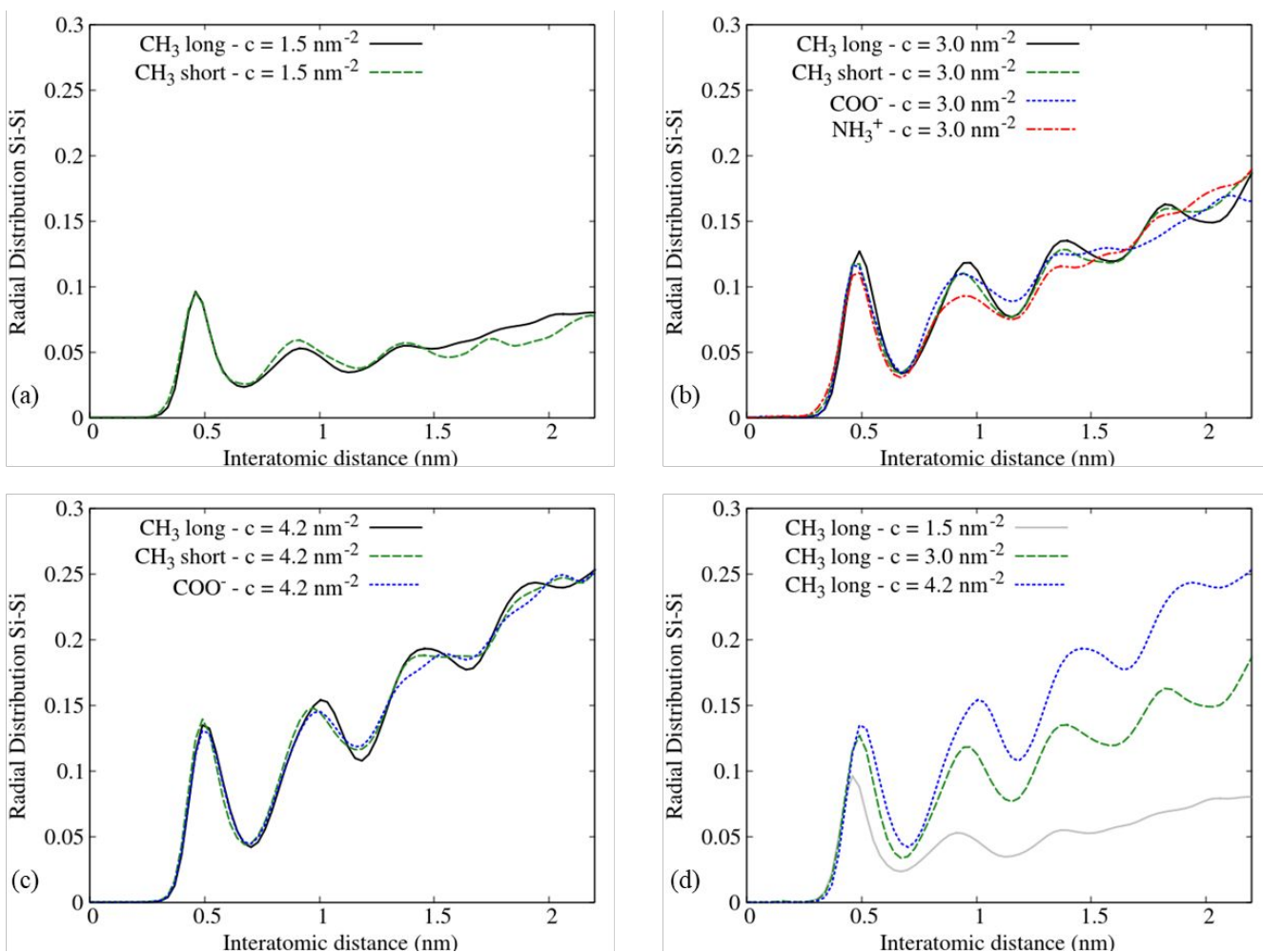


Figure 4. Radial distribution functions (RDF) of silane monolayers at different surface coverages: (a) $c = 1.5 \text{ nm}^{-2}$, (b) $c = 3.0 \text{ nm}^{-2}$, (c) $c = 4.2 \text{ nm}^{-2}$ and (d) CH_3 long at different coverages after 100 ns MD simulation. The peaks observed at a periodic interatomic distance show that a positional order appears in the silane monolayers.

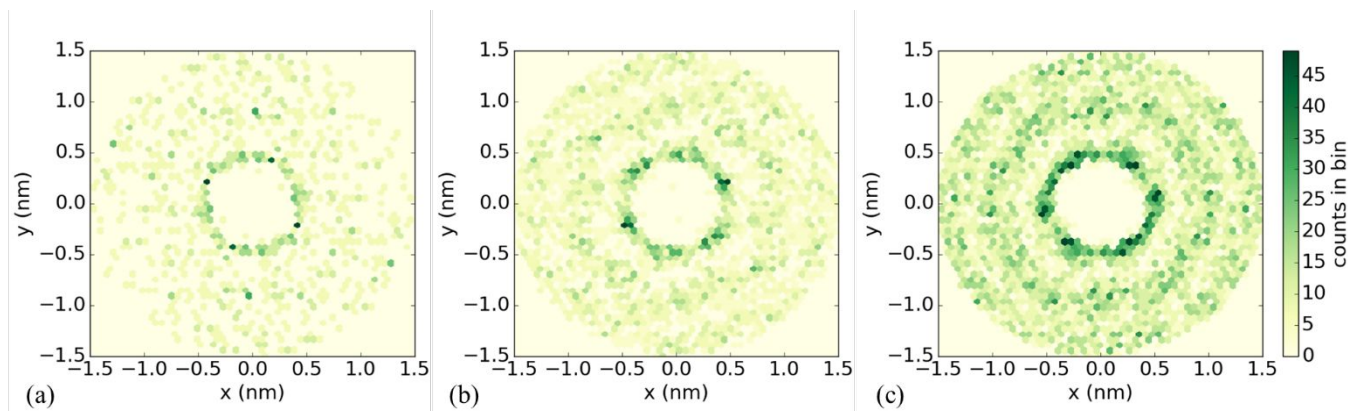


Figure 5. Two-dimensional Si – Si radial distribution functions of CH₃ long silane monolayer at different surface coverages (arbitrary units): (a) $c = 1.5 \text{ nm}^{-2}$, (b) $c = 3.0 \text{ nm}^{-2}$ and (c) $c = 4.2 \text{ nm}^{-2}$. A hexagonal positional order appears when surface coverage of alkylsilane molecules increases.

Moreover, our results show that, whatever the monolayer studied, independently of alkyl chain length and head-group charge, the first peak (*i.e.* lattice parameter, minimum Si-Si distance between two neighboring molecules) is shifted towards higher values as surface coverage increases, reaching 0.45 nm at $c = 1.5 \text{ nm}^{-2}$, 0.49 nm at $c = 3.0 \text{ nm}^{-2}$, and 0.5 nm at $c = 4.2 \text{ nm}^{-2}$. This result can be explained by the flexibility of the alkyl chains. Indeed, their higher flexibility at low surface coverage could allow Si atoms from silane molecules to position themselves closer to each other, during the diffusion phase of the MD simulation, while respecting the Van der Waals radius of the Si atom (which is 0.21 nm). For a given surface coverage, the intensity of the first peak is the same whatever the system. It means that the number of closest neighbor silane molecules does not depend on alkyl chain length and on charged head-groups. For CH₃ short and CH₃ long molecules at $c = 3.0 \text{ nm}^{-2}$ and $c = 4.2 \text{ nm}^{-2}$, the RDF shows that the hexagonal packing persists on the (x,y) plane, up to 2 nm around the origin as four peaks are well-defined on Figure 4. It is not the case for charged head-groups, only the two first peaks are visible meaning that the

propagation of the hexagonal packing is limited up to 1.5 nm. Consequently, NH_3^+ and COO^- silane monolayers are more disordered than CH_3 short and CH_3 long monolayers.

To conclude, the persistence length of the hexagonal packing can be correlated with the nematic order parameter, as it increases with surface coverage, it is independent of chain length and tilt angle distribution, and it is prevented by charged head-groups. Thus, among the four investigated silane monolayers, it seems that CH_3 long and CH_3 short monolayers at coverages $c = 3 \text{ nm}^{-2}$ and $c = 4.2 \text{ nm}^{-2}$, lead to the highest positional order. However, CH_3 short silane molecules have a larger tilt angle distribution than CH_3 long silane molecules. Also, the persistence length of the hexagonal packing seems to be related to the degree of aggregation on the surface observed on Figure 1. Indeed, for a coverage of 3.0 nm^{-2} , four peaks are well-defined on the RDF plots for CH_3 long and CH_3 short monolayers, while only two peaks are well-defined for NH_3^+ and COO^- monolayers (Figure 4b). This result suggests that the persistence length of the hexagonal packing increases with the degree of aggregation of silane molecules.

2.2. Experimental validation of the simulated morphology

Previous experimental studies have shown that molecules with long alkyl chains are more ordered, they present smaller tilt angles, and are more densely packed on surface than molecules with short alkyl chains.^{11,12,35-37} Most of the experimental studies are focused on multifunctional silane molecules, allowing silane cross-linking, whereas in the MD simulations monofunctional silane molecules are used. The monolayer morphology depends on the nature of silane molecules.³⁶ So, to check that our simulation results are consistent with experiments, FTIR-ATR analysis were carried out to qualitatively compare the alkyl chain tilt angle of the NH_3^+ , COO^- , CH_3 short and CH_3 long monolayers. The surface coverages were estimated by XPS measurements.

XPS analysis. XPS survey spectra of the bare SiO₂/Aluminium/Silicon substrate, and of the four silanized SiO₂/Aluminium/Silicon substrates are shown on Figures S4 - S8 (Supporting Information). The bare substrate shows distinct O1s and Si2p peaks, while C1s is not detected. Silanized substrates show distinct C1s, O1s and Si2p peaks, their binding energies are reported in Table S1 (Supporting Information). C1s, O1s, and Si2p core levels are shown on Figure S5 – S8 (Supporting Information). Two contributions are present in the high resolution Si2p spectra for the silanized substrates, which are associated to Si(-O)₄ and to Si(-O)₁ (Table S1, Supporting Information). The Si(-O)₄ contribution is consistent with the silicon associated with oxygen in the silica substrate. The presence of Si(-O)₁ contribution comforts the success of the silanization. Indeed, the four silanes used in this study are monovalent. The atomic percentages of the bare substrate and of the four silanized substrates are reported in Table S1 (Supporting Information). The Si:O ratio is about 1.6 for each substrate. The Si(-O)₄:C ratio is consistent with the silane molecular composition, except for CH₃ short monolayer. Indeed, carbon contamination appears systematically on CH₃ short monolayer, although the silane solution is not contaminated.

The surface coverage of silanes, $\Gamma_{silanes}$, is estimated from the formula:³⁸

$$\Gamma_{silanes} = \frac{A_{Si(-O)_1}}{A_{Si2p}} n_{SiO_2} z$$

where $A_{Si(-O)_1}$ and A_{Si2p} are the normalized area of the Si(-O)₁ peak and of (Si(-O)₁ + Si(-O)₄) components respectively, n_{SiO_2} is the molecular concentration of silica (22 nm⁻³) and z is the sampling depth. z is approximated by 3λ , with λ is the mean free path in silica, equal to 3.7 nm.^{39,40} The surface coverages are about 3 nm⁻² for CH₃ short, CH₃ long, and COO⁻ monolayers, and around 8 nm⁻² for NH₃⁺. So, contrary to previous results obtained for multifunctional silanes¹², the

coverage does not depend on the alkyl chain length. The NH_3^+ surface coverage is more than two times higher than the surface coverage obtained with the other silane molecules. It might be explained by the catalytic effect of amino groups during silanization process.^{41,42} Also, it is worth to be noticed that, because of sampling depth and variations in alkyl chain length, the calculation underestimates the ratio between the surface coverage of short alkyl chains (CH_3 short or NH_3^+) and long alkyl chains (CH_3 long or COO^-).

FTIR-ATR analysis. It is well-known that the methylene asymmetric stretching mode is shifted to the lower frequency region as the alkyl chain order increases.^{11,17,43,44} Moreover, several studies combining infrared spectroscopy, ellipsometry and AFM show that an increase in the alkyl chain order, or a shift to lower frequency region, is associated with a decrease in the alkyl chain tilt angle.^{12, 44}

The FTIR-ATR spectra of the COO^- , CH_3 long and NH_3^+ monolayers, shown in Figure 6, are dominated by the methylene symmetric stretching mode (d^+ , in the range 2854 cm^{-1} - 2858 cm^{-1}) and the methylene asymmetric stretching (d^- , in the range 2924 cm^{-1} - 2928 cm^{-1}) mode. These modes are not observed on the CH_3 short monolayer, likely because the CH_3 short molecule has fewer methylene groups than the CH_3 long and COO^- molecules. However, despite NH_3^+ and CH_3 short molecules have the same number of methylene groups, d^+ and d^- modes are observed on the NH_3^+ monolayer. It can be explained by the higher surface coverage obtained with NH_3^+ molecules than with CH_3 short molecules (8 nm^{-2} vs. 3 nm^{-2}). Our results show a shift to low frequencies, by up to 4 cm^{-1} , for d^- modes of CH_3 long (2929 cm^{-1}), NH_3^+ (2927 cm^{-1}), and COO^- (2925 cm^{-1}) monolayers. Such a shift suggests a higher tilt angle for CH_3 long than for NH_3^+ and COO^- monolayers.⁴⁴ These results are in agreement with our tilt angles obtained by MD simulation. Indeed, the tilt angle of CH_3 long molecules at a coverage of 3.0 nm^{-2} is 34° , while the tilt angle

of NH_3^+ molecules at a coverage of 4.2 nm^{-2} and the one of COO^- at a coverage of 3.0 nm^{-2} are close, around 12° - 19° (Supporting Information, Figure S2).

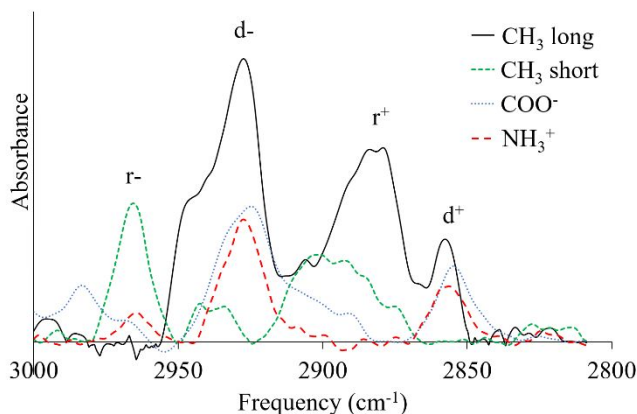


Figure 6. FTIR-ATR spectra of the four silanized surfaces.

The methyl asymmetric stretching mode (r^- in plane, 2966 cm^{-1}) is clearly resolved on the CH_3 short monolayer only, while the methyl symmetric stretching (r^+ , 2878 cm^{-1} and r^+ FR 2940 cm^{-1}) is clearly resolved on CH_3 long monolayer, but not on CH_3 short monolayer. Such results have already been observed from polarized FTIR-ATR experiments.¹² In polarized FTIR-ATR experiments, the r^- mode is observed only if the alkyl chains are nearly perpendicular to the surface, while the r^+ mode is observed for alkyl chains with higher tilt angles only. In the present study, we cannot calculate the different tilt angles because we use an unpolarized FTIR-ATR equipment. However, our results suggest that a change in orientation occurs between CH_3 long and CH_3 short molecules. Indeed as surface coverage is the same for CH_3 short and CH_3 long monolayers, if there were no change in the average alkyl chain tilt angle, then the r^- and r^+ peak areas of these two monolayers would be the same (with different widths, depending on the tilt angle distribution). By assuming that the presence of the r^- mode on the CH_3 short system is not entirely linked to the carbon contamination, these experimental results are qualitatively in agreement with tilt angles

from our MD simulations, which suggest that the tilt angle of CH₃ long molecules is 34° while the one of CH₃ short molecules is 22°.

Previous experimental studies have shown that, in the case of multifunctional silane molecules, the surface coverage increases, and the tilt angle decreases, as the alkyl chain length increases.¹² Our experimental and simulated results suggest that, in the case of monofunctional silane molecules, likely because of the absence of intermolecular bonds, the alkyl chain length has no significant effect on the surface coverage. However, the average chain tilt angle increases as the chain length increases.

3. Conclusion

This study shows that the ordered state of the silane monolayer depends on the alkyl chain length (n from 3 to 18), head-group charge, and on the surface coverage. Indeed, long alkyl chains and high coverages lead to more organized self-assembled silane monolayers, with a narrow tilt angle distribution centered on a preferred orientation, and few gauche distortions. Also, for given alkyl chain length and surface coverage, charged silane molecules lead to a more disordered state than neutral silane molecules, with a larger tilt angle distribution. Long alkyl chains ($n > 8$) were reported to have a tilt angle independent of chain length and to be affected by surface coverage. On the contrary, short alkyl chains ($n = 3$) behave very differently, since their tilt angle seems to be independent from surface coverage. Furthermore, a charged head-group seems to influence the tilt angle to surface coverage relationship of long alkyl chain ($n > 8$). Indeed no influence of surface coverage on the COO⁻ ($n = 11$) tilt angle was observed. The differences between the simulated tilt angles, depending on the nature of silane molecules, are validated by FTIR-ATR analysis.

Moreover, our results suggest that a hexagonal packing is observed in all the studied silane monolayers. However, whatever the alkyl chain length, an increase in surface coverage lead to the more marked appearance of the hexagonal packing. Nematic order parameter values show that such packing is governed by the parallel orientation of the first C-C bonds of the silane molecules, near the SiO₂ surface. Thus, even short alkyl chain (CH₃ short), despite a large tilt angle distribution, present a well-defined hexagonal packing at high coverage.

Surface chemical functionalization is used in analytical tools as a mean to immobilize biomolecules that will capture a specific analyte, but also to reduce the non-specific adsorption. This work could further help to understand the influence of the nature of silane molecules on the arrangement of the silane monolayer on SiO₂ surfaces, and on subsequent biomolecule interactions, to design more efficient analytical tools.

ASSOCIATED CONTENT

The following files are available free of charge.

Diffusion distance of silane molecules. Tilt angle distributions. Sub-coverages for each system studied at 3 nm⁻² and 1.5 nm⁻². Radial distribution functions of CH₃ long silane molecules. XPS spectra. XPS binding energy and atomic percentages. (PDF)

AUTHOR INFORMATION

Corresponding Author

*Email: christelle.yeromonahos@ec-lyon.fr

Author Contributions

The manuscript was written through contributions of all authors. All authors have given approval to the final version of the manuscript.

Funding Sources

This work was supported by the Young Researcher ANR PORIDG project, grant ANR-18-CE09-0006 of the French Agence Nationale de la Recherche. This work was granted access to the HPC resources of CINES under the allocation 2019-A0070711100 made by GENCI. Also, this work was supported by the PMCS2I - supercomputer Newton from Ecole Centrale de Lyon, France, member of the FLMSN.

ACKNOWLEDGMENT

The authors thank Laurent Pouilloux, Anne Cadiou, and Laurent Carrel for support on PMCS2I resources.

REFERENCES

- (1) Beaucage, S. L. Strategies in the preparation of DNA oligonucleotide arrays for diagnostic applications. *Curr. Med. Chem.* **2001**, *8*, 1213-1244.
- (2) Beier, M.; Hoheisel, J. D. Versatile derivatisation of solid support media for covalent bonding on DNA-microchips. *Nucleic Acids Res.* **1999**, *27*, 1970-1977.
- (3) Wang, Y.; Cai, J.; Rauscher, H.; Behm, R. J.; Goedel, W. A. Maleimido-Terminated Self-Assembled Monolayers. *Chem. Eur. J.* **2005**, *11*, 3968-3978.

- (4) Luderer F.; Walschus U. Immobilization of Oligonucleotides for Biochemical Sensing by Self-Assembled Monolayers: Thiol-Organic Bonding on Gold and Silanization on Silica Surfaces. *Wittmann C. (eds) Immobilisation of DNA on Chips I. Topics in Current Chemistry Springer, Berlin Heidelberg* **2005**, 260, 37-56.
- (5) Hitaishi, V. P. ; Clement, R. ; Bourassin, N. ; Baaden, M. ; De Poulpiquet, A. ; Sacquin-Mora, S. ; Ciaccafava, A. ; Lojou, E. Controlling redox enzyme orientation at planar electrodes. *Catalysts* **2018**, 8, 192.
- (6) Ruan, M.; Seydou, M.; Noel, V.; Piro, B.; Maurel, F.; Barbault, F. Molecular dynamics simulation of a RNA aptasensor. *J. Phys. Chem. B* **2017**, 121, 4071-4080.
- (7) Chu-jiang, C.; Zhi-gang, S.; Yu-shan, X.; Shu-lin, M. Surface topography and character of γ -aminopropyltriethoxysilane and dodecyltrimethoxysilane films adsorbed on the silicon dioxide substrate via vapour phase deposition. *J. Phys. D: Appl. Phys.* **2006**, 39, 4829-4837.
- (8) Halliwell, C. M.; Cass, A. E. A factorial analysis of silanization conditions for the immobilization of oligonucleotides on glass surfaces. *Anal. Chem.* **2001**, 73, 2476-2483.
- (9) Al-Hajj, N.; Mousli, Y.; Miche, A.; Humblot, V.; Hunel, J.; Heuzé, K.; Buffeteau, T.; Genin, E.; Vellutini, L. Influence of the Grafting Process on the Orientation and the Reactivity of Azide-Terminated Monolayers onto Silica Surface. *Appl. Surf. Sci.* **2020**, 146778.
- (10) Britt, D. W.; Hlady, V. An AFM study of the effects of silanization temperature, hydration, and annealing on the nucleation and aggregation of condensed OTS domains on mica. *J. Colloid Interface Sci.* **1996**, 178, 775-784.

- (11) Yeon, H.; Wang, C.; Van Lehn, R. C.; Abbott, N. L. Influence of Order within Nonpolar Monolayers on Hydrophobic Interactions. *Langmuir* **2017**, *33*, 4628-4637.
- (12) Barrett, A.; Petersen, P. B. Order of dry and wet mixed-length self-assembled monolayers. *J. Phys. Chem. C* **2015**, *119*, 23943-23950.
- (13) Steinrück, H. G.; Will, J.; Magerl, A.; Ocko, B. M. Structure of n-Alkyltrichlorosilane Monolayers on Si (100)/SiO₂. *Langmuir* **2015**, *31*, 11774-11780.
- (14) Wen, K.; Maoz, R.; Cohen, H.; Sagiv, J.; Gibaud, A.; Desert, A.; Ocko, B. M. Postassembly chemical modification of a highly ordered organosilane multilayer: New insights into the structure, bonding, and dynamics of self-assembling silane monolayers. *ACS nano* **2008**, *2*, 579-599.
- (15) Koga, T.; Honda, K.; Sasaki, S.; Sakata, O.; Takahara, A. Phase transition of alkylsilane monolayers studied by temperature-dependent grazing incidence X-ray diffraction. *Langmuir* **2007**, *23*, 8861-8865.
- (16) Ito, Y.; Virkar, A. A.; Mannsfeld, S.; Oh, J. H.; Toney, M.; Locklin, J.; Bao, Z. Crystalline ultrasmooth self-assembled monolayers of alkylsilanes for organic field-effect transistors. *J. Am. Chem. Soc.* **2009**, *131*, 9396-9404.
- (17) Naik V.V.; Städler R.; Spender N.D. Effect of leaving group on the structures of alkylsilane SAMs. *Langmuir* **2014**, *30*, 14824-14831.
- (18) Roscioni, O. M.; Muccioli, L.; Mityashin, A.; Cornil, J.; Zannoni, C. Structural characterization of alkylsilane and fluoroalkylsilane self-assembled monolayers on SiO₂ by molecular dynamics simulations. *J. Phys. Chem. C* **2016**, *120*, 14652-14662.

- (19) Castillo, J. M.; Klos, M.; Jacobs, K.; Horsch, M.; Hasse, H. (2015). Characterization of alkylsilane self-assembled monolayers by molecular simulation. *Langmuir* **2015**, *31*, 2630-2638.
- (20) Black, J. E.; Iacovella, C. R.; Cummings, P. T.; McCabe, C. Molecular dynamics study of alkylsilane monolayers on realistic amorphous silica surfaces. *Langmuir* **2015**, *31*, 3086-3093.
- (21) Black, J. E.; Summers, A. Z.; Iacovella, C. R.; Cummings, P. T.; McCabe, C. Investigation of the Impact of Cross-Polymerization on the Structural and Frictional Properties of Alkylsilane Monolayers Using Molecular Simulation. *Nanomaterials* **2019**, *9*, 639.
- (22) Ewers, B.W.; Batteas, J.D. Molecular dynamics simulations of alkylsilane monolayers on silica nanoasperities: impact of surface curvature on monolayer structure and pathways for energy dissipation in tribological contacts. *J. Phys. Chem. C* **2012**, *116*, 25165-25177.
- (23) Dugas, V.; Depret, G.; Chevalier, Y.; Nesme, X.; Souteyrand, É. Immobilization of single-stranded DNA fragments to solid surfaces and their repeatable specific hybridization: covalent binding or adsorption? *Sens. Actuator B-Chem.* **2004**, *101*, 112-121.
- (24) Lecot S.; Chevolot Y.; Phaner-Goutorbe M.; Yeromonahos C. Impact of silane monolayers on the adsorption of streptavidin on silica and its subsequent interactions with biotin: molecular dynamics and steered molecular dynamics simulations. *J. Phys. Chem. B* **2020**, *124*, 6786-6796.
- (25) Roscioni, O. M.; Muccioli, L.; Della Valle, R. G.; Pizzirusso, A.; Ricci, M.; Zannoni, C. Predicting the anchoring of liquid crystals at a solid surface: 5-cyanobiphenyl on cristobalite and glassy silica surfaces of increasing roughness. *Langmuir* **2013**, *29*, 8950-8958.
- (26) Kitabata, M.; Taddese, T.; Okazaki, S. Molecular dynamics study on wettability of poly(vinylidene fluoride) crystalline and amorphous surfaces. *Langmuir* **2018**, *34*, 12214-12223.

- (27) Van Der Spoel, D.; Lindahl, E.; Hess, B.; Groenhof, G.; Mark, A. E.; Berendsen, H. J. GROMACS: fast, flexible, and free. *J. Comput. Chem.* **2005**, *26*, 1701-1718.
- (28) Humphrey, W.; Dalke, A.; Schulten, K. VMD: visual molecular dynamics. *J. Mol. Graph.* **1996**, *14*, 33-38.
- (29) Jorgensen, W. L.; Maxwell, D. S.; Tirado-Rives, J. Development and testing of the OPLS all-atom force field on conformational energetics and properties of organic liquids. *J. Am. Chem. Soc.* **1996**, *118*, 11225-11236.
- (30) Schulze, E.; Stein, M. Simulation of Mixed Self-Assembled Monolayers on Gold: Effect of Terminal Alkyl Anchor Chain and Monolayer Composition. *J. Phys. Chem. B* **2018**, *122*, 7699-7710.
- (31) Anvari, M. H.; Liu, Q.; Xu, Z.; Choi, P. Molecular Dynamics Study of Hydrophilic Sphalerite (110) Surface as Modified by Normal and Branched Butylthiols. *Langmuir* **2018**, *34*, 3363-3373.
- (32) Parikh, A. N.; Allara, D. L.; Azouz, I. B.; Rondelez, F. An intrinsic relationship between molecular structure in self-assembled n-alkylsiloxane monolayers and deposition temperature. *The J. Phys. Chem.* **1994**, *98*, 7577-7590.
- (33) Allara, D. L.; Nuzzo, R. G. Spontaneously organized molecular assemblies. 2. Quantitative infrared spectroscopic determination of equilibrium structures of solution-adsorbed n-alkanoic acids on an oxidized aluminum surface. *Langmuir* **1985**, *1*, 52-66.
- (34) Deetz, J. D.; Ngo, Q.; Faller, R. Reactive Molecular Dynamics Simulations of the Silanization of Silica Substrates by Methoxysilanes and Hydroxysilanes. *Langmuir* **2016**, *32*, 7045-7055.

- (35) Porter, M. D.; Bright, T. B.; Allara, D. L.; Chidsey, C. E. Spontaneously organized molecular assemblies. 4. Structural characterization of n-alkyl thiol monolayers on gold by optical ellipsometry, infrared spectroscopy, and electrochemistry. *J. Am. Chem. Soc.* **1987**, *109*, 3559-3568.
- (36) Ulman, A. Formation and structure of self-assembled monolayers. *Chem. Rev.* **1996**, *96*, 1533-1554.
- (37) Pujari, S. P.; Scheres, L.; Marcelis, A. T. ; Zuilhof, H. Covalent surface modification of oxide surfaces. *Angew. Chem. Int. Ed.* **2014**, *53*, 6322-6356.
- (38) Shircliff, R. A.; Martin, I. T.; Pankow, J. W.; Fennell, J.; Stradins, P.; Ghirardi, M. L.; Cowley, S. W.; Branz, H. M. High-resolution X-ray photoelectron spectroscopy of mixed silane monolayers for DNA attachment. *ACS Appl. Mater. Interfaces* **2011**, *3*, 3285-3292.
- (39) Vickerman, J. C.; Gilmore, I. S. (Eds.) Surface analysis: the principal techniques. *John Wiley & Sons.* **2011**.
- (40) Tanuma, S.; Powell, C. J.; Penn, D. R. Calculations of electron inelastic mean free paths (IMFPS). IV. Evaluation of calculated IMFPS and of the predictive IMFP formula TPP-2 for electron energies between 50 and 2000 eV. *Surf. Interface Anal.* **1993**, *20*, 77-89.
- (41) Kinkel, J. N.; Unger, K. K. Role of solvent and base in the silanization reaction of silicas for reversed-phase high-performance liquid chromatography. *J. Chromatogr. A*, **1984**, *316*, 193-200.
- (42) Fadeev, A. Y.; McCarthy, T. J. Self-assembly is not the only reaction possible between alkyltrichlorosilanes and surfaces: monomolecular and oligomeric covalently attached layers of dichloro- and trichloroalkylsilanes on silicon. *Langmuir* **2000**, *16*, 7268-7274.

(43) Ardès-Guisot, N.; Durand, J. O.; Granier, M.; Perzyna, A.; Coffinier, Y.; Grandidier, B.; Wallart X.; Stievenard, D. Trichlorosilane isocyanate as coupling agent for mild conditions functionalization of silica-coated surfaces. *Langmuir* **2005**, *21*, 9406-9408.

(44) Nam, H.; Granier, M.; Boury, B.; Park, S.Y. Functional organotrimethoxysilane derivative with strong intermolecular $\pi-\pi$ interaction: One-pot grafting reaction on oxidized silicon substrates. *Langmuir* **2006**, *22*, 7132-7134.

For Table of Contents Only

